Generation of a Family of Protein Fragments for Structure–Folding Studies. 2. Kinetics of Association of the Two Chymotrypsin Inhibitor-2 Fragments

Gonzalo de Prat Gay, Javier Ruiz-Sanz,‡ and Alan R. Fersht*

MRC Unit for Protein Function and Design, Department of Chemistry, Cambridge University, Lensfield Road, Cambridge CB2 1EW, U.K.

Received February 21, 1994; Revised Manuscript Received April 19, 1994®

ABSTRACT: The kinetics of association of the fragments of the barley chymotrypsin inhibitor-2, CI-2(20–59) and CI-2(60–83), to form a native-like structure follows two phases. There is a major second-order component with rate constant $(3.7 \pm 0.3) \times 10^3$ M^{-1} s^{-1} and a slow first-order phase of rate constant 0.011 ± 0.001 s^{-1}. The major phase contains a cooperative folding process as judged by the secondary structure recovery in parallel with the fluorescence change. The time course for structure formation has uniform changes at all of the wavelengths of the circular dichroism spectra, suggesting that all elements of secondary structure are formed simultaneously. A series of kinetic experiments suggest that the association and folding occur in the second-order step and that the first-order step probably results from a *cis–trans* peptidyl–prolyl isomerization in the fragment CI-2(20–59). This was confirmed by experiments on fragments derived from two mutants whose parent proteins fold more slowly than wild-type CI-2. Those fragments display lower second-order rate constants, but the rate constants of the first-order phase are the same as for wild type. The experiments suggest that the mechanism of the association/folding of mutant fragments may be studied by a protein-engineering analysis.

It is thought that the folding of proteins is too rapid to proceed by the random searching of conformational space by individual amino acid residues (Levinthal, 1968), and so there must be concerted formation of one or more elements of structure within a protein that somehow act as points of initiation for the formation of the final folded structure (Wetlaufer, 1973). One possibility is that some elements of secondary structure form rapidly and then come together or propagate (Ptitsyn, 1973; Karplus & Weaver, 1976; Kim & Baldwin, 1990).

The tendency of fragments to form a structure similar to the one adopted in the full protein supports the idea of local interactions playing an important role in the early steps of the folding process (Sancho *et al.*, 1992; Dyson *et al*, 1992., Waltho *et al.*, 1993). It was also reported that fragments of proteins can be good models for denatured states in water (Shortle & Meeker, 1989). In this way, the kinetics of complementation of the fragments comprising the full length of a protein may give information about the role of these structures in the time scale of events of protein folding. It is of importance to study the formation of native-like structures from the assembly of fragments since analysis of these individual fragments can give clues about the existence of initiation sites.

Protein fragments can complement each other and refold to give native-like structures as in previously reported cases [Taniuchi & Anfinsen, 1971; Hartley, 1977; see references in Prat Gay and Fersht (1994)]. The ribonuclease barnase folds via a well-characterized folding intermediate (Fersht, 1993). Two fragments of barnase that have small fractions of native-like structure, which also occur in the folding intermediate, associate relatively readily (Sancho & Fersht, 1992; Kippen *et al.*, 1994). CI-2, on the other hand, folds via a perfect two-state mechanism, without any kinetically significant intermediate (Jackson & Fersht, 1991b).

In the present work, we study the association kinetics of the two CI-2 fragments we have generated by cyanogen bromide cleavage and shown to form a native-like structure (Prat Gay & Fersht, 1994). The process is slow, enabling us to monitor to some extent the structural changes involved. A mechanism is suggested for the interaction of the fragments.

EXPERIMENTAL PROCEDURES

Preparation and Purification of the Fragments. Wild-type CI-2 fragments were prepared as described in Prat Gay and Fersht (1994). Mutant fragments IV48CI-2(20–59) and SA31CI-2(20–59) were cleaved from the corresponding intact mutants (Jackson *et al.*, 1993; N. el Masry, unpublished). Residue numbering is according to the full-length protein, the first residue being number 20. The fragments were therefore named CI-2(20–59) and CI-2(60–83). Concentrations of the fragments were determined from the extinction coefficient of tryptophan for CI-2(20–59) and of tyrosine for CI-2(60–83) in model compounds (Gill & von Hippel, 1989).

Association/Folding Monitored by Fluorescence. A Perkin-Elmer LS-5B fluorimeter was used. The indicated concentrations of the fragments in each experiment were mixed in a 1-mL volume of 10 mM Na_2HPO_4 buffer, pH 6.3, at 25 °C (7.75 mM NaH_2PO_4, 2.25 mM Na_2HPO_4). Emission at 356 nm from excitation at 280 nm was measured at time intervals up to 1 h. A control experiment in which the shutter was closed between measurements gave identical results to leaving the shutter open, indicating the absence of artifacts from photolysis. This was further assessed by following the fluorescence change of CI-2(20–59) alone and of the preformed [CI-2(20–59)·(60–83)] complex. Data were analyzed using Kaleidagraph (Abelbeck software) and fitted to the equations described in the Results section. Temperature was monitored continuously using a probe in the cuvette to an accuracy of ±0.1 °C.

Double-Jump Experiment. The folding reaction was performed by mixing the two fragments in 0.5 mL of 10 mM phosphate buffer, pH 6.3 (7.75 mM NaH_2PO_4, 2.25 mM Na_2HPO_4) at 25 °C, at the concentrations indicated in Figure

* To whom correspondence should be addressed.
‡ Recipient of an EEC Fellowship.
® Abstract published in *Advance ACS Abstracts,* June 1, 1994.

0006-2960/94/0433-7964$04.50/0

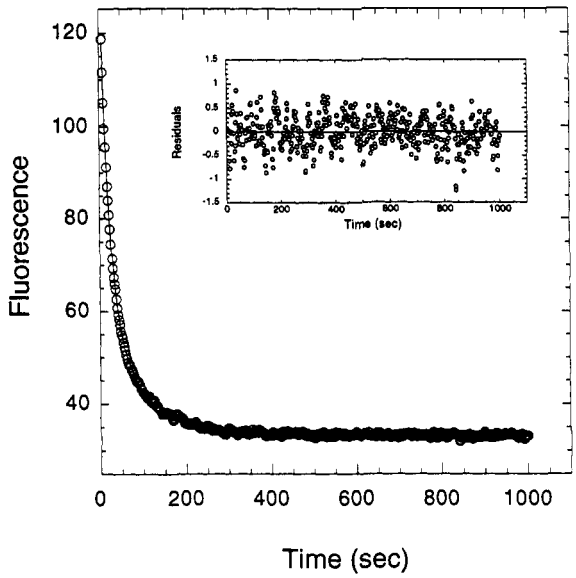

FIGURE 1: Kinetics of association of fragments under pseudo-first-order conditions. CI-2(20–59), 0.5 μM in 10 mM phosphate buffer, pH 6.3 at 25 °C, was mixed with CI-2(60–83) at a final concentration of 10 μM. The data were fitted to a double-exponential decay.

7. The experiment is described in detail in the Results section. For the unfolding/dissociation we used 1.75 M guanidinium chloride (Gdm·Cl), and the fluorescence change was followed at 356 nm (excitation at 280 nm).

Circular Dichroism. For the association/refolding of CI-2(20–59) and CI-2(60–83), the fragments were mixed in a 1-cm path cuvette, and the ellipticity change at 200 nm was measured at time intervals using a Jasco J700 instrument. Below 200 nm the signal is too noisy, and at 210–220 nm the ellipticity change upon refolding is very small. The best signal to noise ratio is obtained at 200 nm. Data points were fitted as described in the Results section. A scan speed of 100 nm/min (two scans) was used for the kinetics of recovery of secondary structure followed by CD spectroscopy. The time for data acquisition is less than 0.7% of the time for the completion of the reaction. Faster scan speeds result in poor-quality spectra.

Stopped-Flow Kinetics. Equal volumes of fragments CI-2(20–59) and CI-2(60–83) were mixed in an Applied Photophysics stopped-flow spectrophotometer, Model SF 17MV. The excitation wavelength was 280 nm, and the emission was ≥315 nm. The fragment association was carried out at pH 6.3 as indicated above and 25.0 °C. The data were analyzed using Kaleidagraph software (Abelbeck Software).

RESULTS

Association Kinetics. Analysis under Pseudo-First-Order Conditions. The initial approach in measuring the rate constant for the association of CI-2(20–59) and CI-2(60–83) fragments was to use pseudo-first-order conditions, i.e., the concentration of CI-2(20–59) was always kept in excess of that of CI-(60–83). Figure 1 shows a typical association/folding curve where the fragment concentration ratio is 1:10. There are two distinguishable phases, and the data fit to a double-exponential process:

$$\Delta F = A_1 \exp(-k_1 t) + A_2 \exp(-k_2 t) + F_\infty \qquad (1)$$

where A_1 and A_2 are the amplitudes of the two phases, k_1 and k_2 represent the rate constants for the two phases, and F_∞ is the end point. In the example of Figure 1, the amplitude of the first process is ~77% of the total change, with $t_{1/2}$ being 13 s; the second process displays an amplitude of ~23% and a $t_{1/2}$ of 60 s. The two processes were then analyzed in the range of 2–40 μM CI-2(60–83) at constant concentrations of CI-2(20–59) (Figure 2). Below 3 μM CI-2(60–83), the two reactions cannot be separated easily because their rates are too similar. At a fixed concentration of 0.5 μM CI-2(20–59), the observed fast rate increases linearly with the increase of added CI-2(60–83) (Figure 2a). The kinetics of this step fit a binding process of

$$\text{CI-2(20–59)} \underset{k_{off}}{\overset{k_{on}[\text{CI-2(60–83)}]}{\rightleftarrows}} \text{[CI-2(20–59)·(60–83)]}$$

which gives as the rate law for the observed rate constant, k_{obs} (k_1),

$$k_1 = k_{off} + k_{on}[\text{CI-2(60–83)}]$$

A value of (3.6 ± 0.2) × 10^3 M^{-1} s^{-1} is obtained for k_{on}, the second-order rate constant. The slower rate constant, k_2, remains constant with the increase of the added fragment with an approximate value of 0.011 s^{-1}, within the analyzed concentration ranges. Figure 2b shows the same process at 2 μM constant CI-2(20–59) with a second-order constant of (3.7 ± 0.3) × 10^3 M^{-1} s^{-1}, in agreement with the value at 0.5 μM. k_2 also shows no variation with concentration at 2 μM CI-2(20–59), with a first-order rate constant of 0.011 ± 0.1 s^{-1}. The same values were obtained at 1 μM (not shown). The value of k_{off} is difficult to obtain with accuracy because there is too long an extrapolation from the linear plots of k_1 versus [CI-2(60–83)]. It is not possible to go to very low [CI-2(60–83)] since the k_2 step (0.011 s^{-1}) interferes. Values of (5.2 ± 2.5) × 10^{-3} and (10 ± 5.0) × 10^{-3} s^{-1} obtained for k_{off} from the data in Figure 2 are too close to 0 for reliable analysis.

In the variation of the relative amplitudes with the increase in [CI-2(60–83)] (Figure 2c,d), we find that the first phase reaches an amplitude of ~80%, and the second, ~20%, of the total amplitude. At low [CI-2(60–83)], the two processes become mixed and the amplitudes consequently change. The lower concentration points are not actually pseudo-first-order, but they do not affect the value of k_{on} in such conditions.

Association of Equimolar Concentrations of Fragments. Concentration Dependence of the Rates. The association reaction was also measured under second-order conditions of [CI-2(20–59)] = [CI-2(60–83)]. At high concentration of fragments, the second-order phase occurs on a faster time scale and so the data can be analyzed by a second-order equation plus an exponential phase as follows. When $[W]_0 = [Y]_0$ (Fersht, 1985),

$$1/([W]_0 - [W{\cdot}Y]) - 1/[W]_0 = k_{on}t \qquad (2)$$

where $[W]_0$ is the initial concentration of CI-2(20–59), $[Y]_0$ is the initial concentration of CI-2(60–83), W·Y is the product of the binding, i.e., the complex, and k_{on} is the second-order rate constant. The equation can be solved for $[W]_0$ to give eq 3:

$$F = F_0 + \{\Delta F[W]_0^2 k_{on}t/(1 + [W]_0 k_{on}t)\} \qquad (3)$$

where F is the fluorescence at time t, and F_0 is the fluorescence at $t = 0$. Figure 3 shows the fluorescence change upon association of CI-2(20–59) and CI-2(60–83), 5 μM concentration of each fragment. Analysis of the data using eq 3 reveals a second-order rate constant, k_{on}, of (3.8 ± 0.1) × 10^3

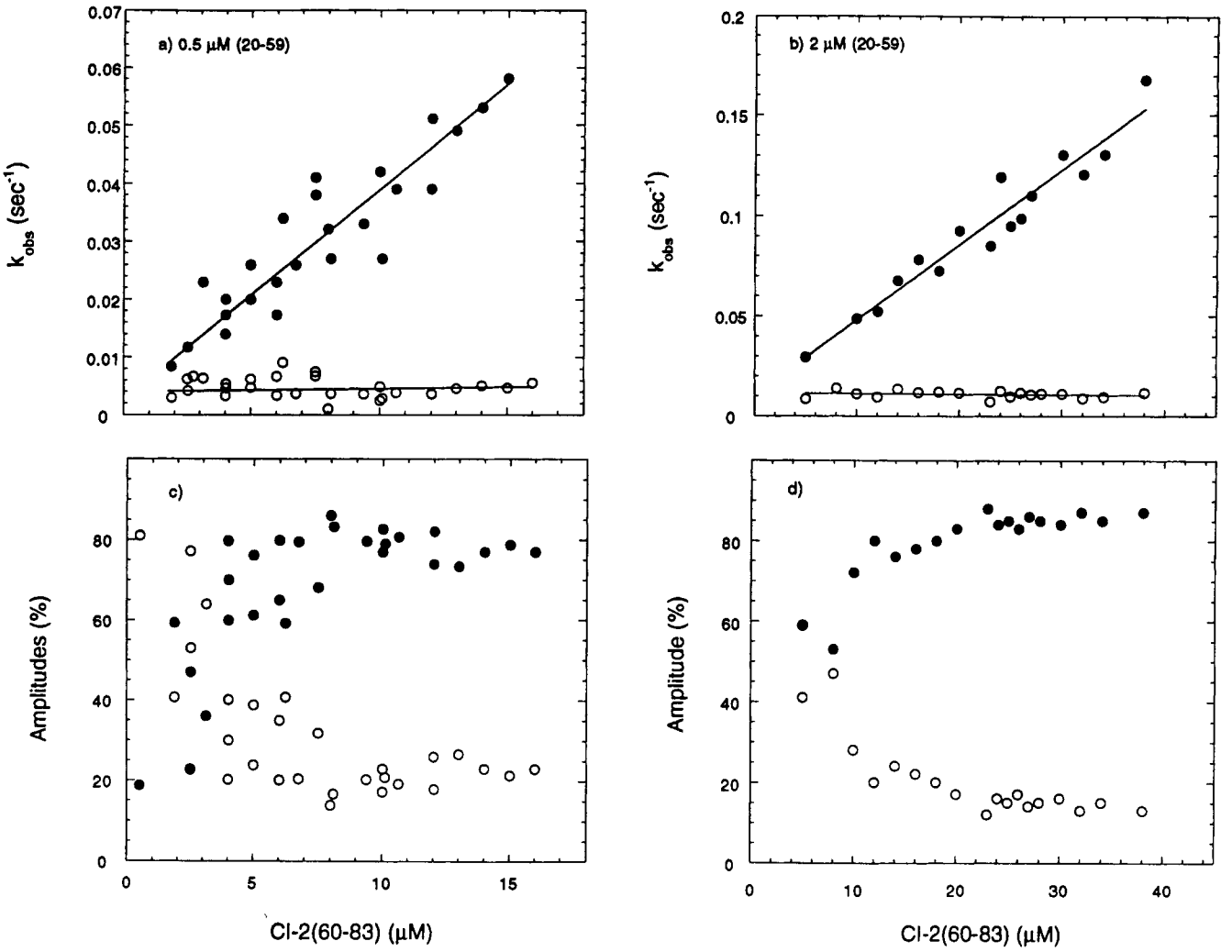

FIGURE 2: Effect of CI-2(60–83) concentration on the rate of formation of the complex under pseudo-first-order conditions. The two-exponential rates obtained (Figure 1, legend) were plotted against concentration of CI-2(60–83) at (a) 0.5 and (b) 2 μM constant [CI-2(20–59)]. Panels c and d are plots showing the relative amplitudes at 0.5 and 2 μM, respectively. It should be noted that the very low concentration points are not strictly in pseudo-first-order conditions. They do not affect the value of k_{on}, and the corresponding amplitudes show when the reaction is under such conditions.

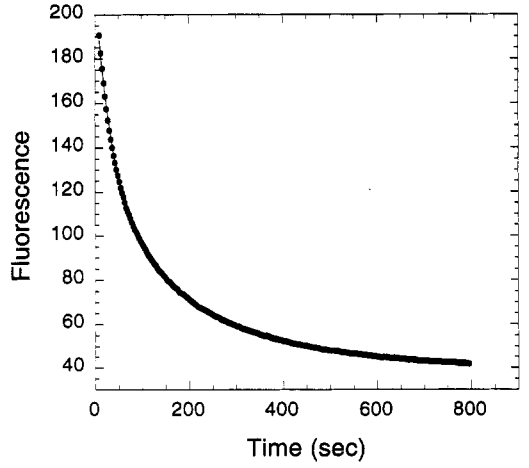

FIGURE 3: Kinetics of association of fragments at equimolar concentrations. The fragments were mixed in equimolar 5 μM concentration in 10 mM phosphate buffer at 25 °C. The data were fitted to eq 3 to obtain the second-order rate constant.

M^{-1} s^{-1}, for initial concentrations of each fragment varying from 0.3 to 30 μM (not shown). The k_{on} determined in this way is independent of the concentration.

The rate constant for the slow phase could perhaps involve proline isomerization (Brandts *et al.*, 1975; Schmid, 1992). Further, two proline isomerizations have been reported in the uncleaved CI-2 slow refolding mechanism (Jackson & Fersht, 1991b). However, catalysis of this step by peptidyl–prolyl isomerase (PPIase) was not observed. It is possible that the structure present in CI-2(20–59) blocks the access of PPIase to the proline bond (Lang *et al.*, 1987; Lin *et al.*, 1988).

Kinetics of Complex Formation. Fluorescence vs Ellipticity Change. The fluorescence experiments described so far report on the formation of tertiary structure around Trp-24. Uncleaved CI-2 has a highly cooperative transition of folding and unfolding, so the fluorescence change is a probe of overall structure (Jackson & Fersht, 1991a). The formation of secondary structure on mixing both fragments was probed by following the time change in ellipticity. Figure 4 shows the change in ellipticity of a 5 μM 1:1 ratio of fragments at 200 nm that monitors the association of the CI-2[(20–59)·(60–83)] complex, together with the fluorescence change. The ellipticity data were fitted using eq 3, and the value obtained for k_{on} was $(3.6 \pm 0.3) \times 10^3$ M^{-1} s^{-1}, the same as from the change in fluorescence. A slow phase was also observed by CD with a rate constant of ~ 0.006 s^{-1}, also in agreement with fluorescence; nevertheless an exact value cannot be determined. Similar changes in ellipticity were observed at 193, 196, and 204 nm (not shown).

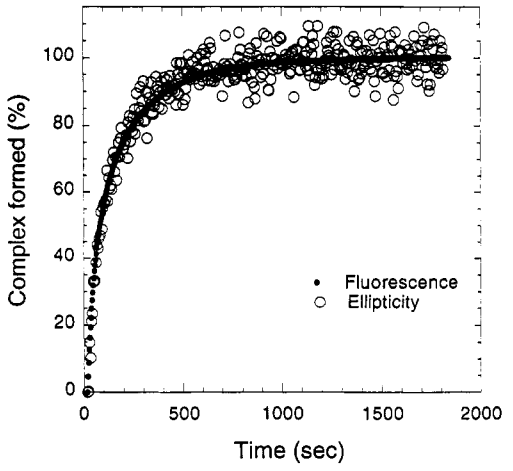

FIGURE 4: Secondary and tertiary structure formation of the complex followed kinetically. Fragments CI-2(20–59) and CI-2(60–83) were mixed at 5 μM each, using the conditions of Figure 3. The fluorescence change was followed at 356 nm, and the ellipticity, at 200 nm.

Kinetics of Structure Formation of the Complex Followed by Circular Dichroism Spectra. Formation of the CI-2[(20–59)·(60–83)] complex gives a structure similar to that of the native full CI-2, as judged from CD and ^{1}H-NMR spectra (Prat Gay & Fersht, 1994). The association of fragments is sufficiently slow that the recovery of overall secondary structure may be easily measured at a single wavelength (Figure 4). The reaction can be slowed down by decreasing the pH to 4.5 and the temperature to 4 °C; in these conditions k_{on} is 180 M^{-1} s^{-1}, 20-fold slower than at pH 6.3 and 25 °C (Figure 5a). We measured the far-UV circular dichroism spectra of the complex as it formed under the same reaction conditions (Figure 5b). The recovery of secondary structure seems to be uniform for all of the regions in the spectra, suggesting that all of the secondary structure elements are formed at the same time. The larger change occurs between 190 and 210 nm; a shift in the minimum from 202 to 207 nm is also observed.

Determination of the Rate Constant for Dissociation of the Complex by Guanidinium Chloride Denaturation/Dissociation. The [CI-2(20–59)·(60–83)] complex can be dissociated/denatured using Gdm·Cl; the process shows a large increase in fluorescence and is completed at approximately 2 M denaturant. Unlike the association process, it displays a single-exponential behavior (not shown). The complex, at a final concentration of 1 μM, was unfolded/dissociated at concentrations of Gdm·Cl between 1.2 and 1.8 M. The logarithm of the rate constant changes linearly with the concentration of denaturant (Figure 6). Extrapolation of the data to water gives a value of (4.0 ± 0.1) × 10^{-4} s^{-1} corresponding to the rate constant for dissociation/denaturation of the complex. The same value for the rate constant was found for the denaturation/dissociation of 5 μM complex.

Double-Jump Folding/Unfolding of the Complex. As described above, the association of [CI-2(20–59)·60–83)] from its component fragments in aqueous solution is a slow process involving at least two phases. A double-jump experiment was performed to follow the formation of fully folded complex. The fragments were mixed at 2 μM concentration each in a 0.5-mL volume and allowed to associate/fold. At the indicated times, 0.5 mL of a 2-fold-concentrated Gdm·Cl solution in the same buffer was mixed into the cuvette and the fluorescence change was monitored (Figure 7). The unfolding was a single-exponential process, and the amplitudes were plotted against time of folding as Figure 8 shows. The absence of a lag at the beginning of the curve indicates that no partially folded (W·Y) intermediate complexes accumulate under the experimental conditions. The amplitudes of the association/folding plotted against time in Figure 7 give a second-order rate constant of (4.2 ± 0.5) × 10^3 M^{-1} s^{-1}, in excellent agreement with the rate constant determined from fluorescence change directly. At time 0, 5% of the molecules are fully folded within the dead time of the experiment (Figure 8, inset) [cf. Kiefhaber *et al.* (1990)]. As a control experiment, we mixed each individual fragment with Gdm·Cl, and no fluorescence change with time was observed. Nevertheless, no fluorescence change could be detected by stopped flow in the 0–200-ms scale (not shown), suggesting that the reaction is too fast or it does not yield a fluorescence change.

Fragment Association at Excess CI-2(20–59) over CI-2(60–83). Determination of the Nature of the Slow Minor Phase. Understanding the nature of the slow minor phase in the association kinetics of the fragments is crucial for unraveling the mechanism. Proline isomerization was shown

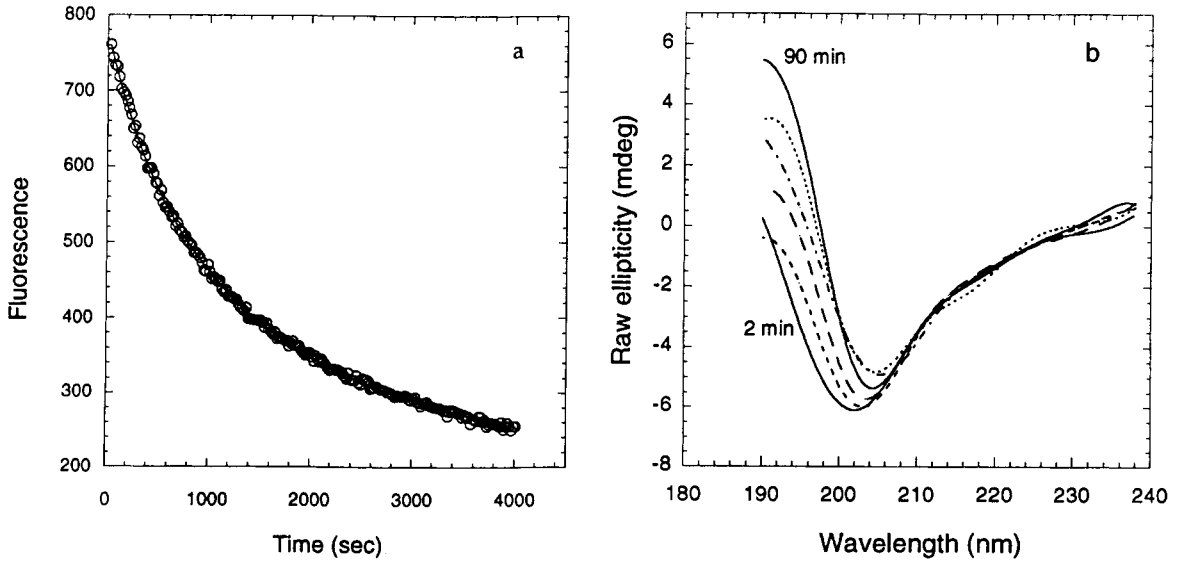

FIGURE 5: Kinetic recovery of the circular dichroism spectra of [CI-2(20–59)·(60–83)]. (a) Fluorescence change of fragment association in sodium acetate buffer, pH 4.5 and 4 °C. (b) CD spectra at different times (2–90 min) in the conditions of panel a (see Experimental Procedures). Fragment concentration was 5 μM of each.

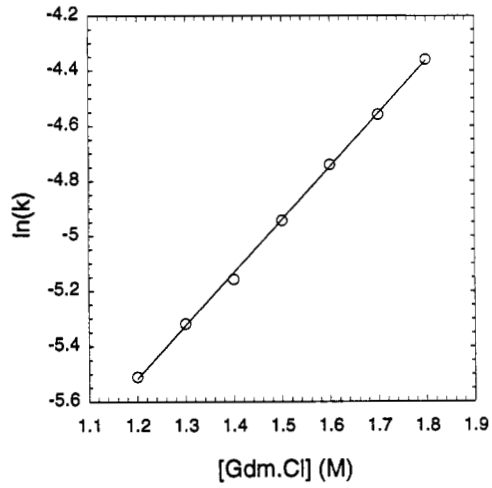

FIGURE 6: Determination of the overall dissociation rate constant of the complex using Gdm·Cl. The fragments were mixed at a concentration of 50 μM in 10 mM phosphate buffer, pH 6.3 at 25 °C. After 30 min, the complex was diluted to 1 μM at the indicated Gdm·Cl concentrations in the same buffer. The data of the fluorescence increase were fitted to single-exponential decays, and the rate constants plotted as shown. The rate constants are in s^{-1}.

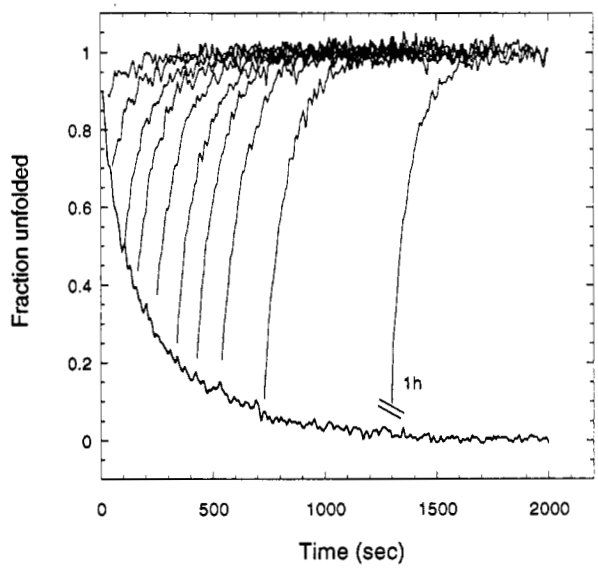

FIGURE 7: Double-jump association/folding–dissociation/unfolding experiment. The fragments were mixed in equimolar concentrations at 2 μM in 10 mM phosphate buffer, pH 6.3 and 25 °C (fluorescence decrease). At different times, the complex was dissociated/denatured by diluting it one-half in Gdm·Cl (3.5 M) in buffer, so that the final concentrations were 1 μM complex and 1.75 M Gdm·Cl (fluorescence increase). After 1 h, the fragments were completely folded; the unfolding of the complex is denoted by a break in the plot.

to give rise to two additional phases in the refolding of uncleaved CI-2 (Jackson & Fersht, 1991b). Of the four prolines present in CI-2, the best candidates are Pro-25 and Pro-44, which are located in CI-2(20–59). Assuming the existence of two populations of proline isomers in CI-2(20–59), in the presence of 10-fold excess CI-2(60–83) both populations will react, giving a two-phase kinetic process (Figure 2). If we reverse the situation and use 10-fold excess CI-2(20–59) over CI-2(60–83), the latter would react preferentially with the population of CI-2(20–59) in the "correct" conformation, yielding a single-exponential phase of association. To test this hypothesis, we analyzed by stopped-flow kinetics a 2.5:25 μM ratio of [CI-2(20–59)]/[CI-2(60–83)] and vice versa as a control (Figure 9). The rate constants obtained are the same: when CI-2(20–59) is in excess (Figure

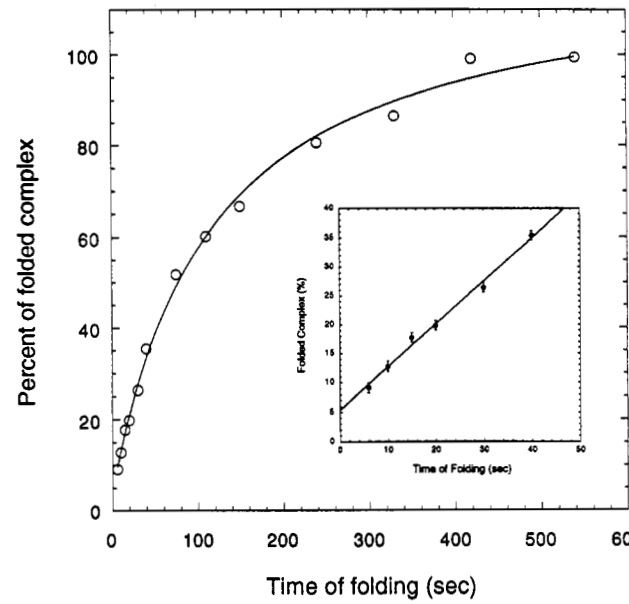

FIGURE 8: Increase of the unfolding amplitudes in the double-jump experiment. Each of the unfolding curves was fitted to a single-exponential decay with a rate constant of 0.009 s^{-1} for all of the time points, and the amplitudes were plotted against time of association/folding. The completion of the folding reaction (100%) was corroborated after dissociation/unfolding of the 1 h association point. The theoretical curve for the amplitudes corresponds to eq 3. The inset represents the extrapolation to time 0 for the determination of the percentage of fast-folding complex.

9a), k_{1obs} is 0.094 ± 0.0005; when CI-2(60–83) is in excess (Figure 9b), k_{1obs} is 0.100 ± 0.0009. Indeed if CI-2(20–59) is the one in excess, the process fits a single-exponential decay as the residuals plot in Figure 9a indicates. Under the same conditions, in the presence of an excess of CI-2(60–83) over CI-2(20–59) the process is clearly not a single-exponential decay (Figure 9b); it corresponds to a double-exponential process as in Figure 1.

Kinetics of Association of Two Mutant Fragments. In order to confirm the nature of the slow first-order phase, we analyzed the pseudo-first-order association of two mutant fragments, IV39CI-2(20–59) and SA31CI-2(20–59), with CI-2(60–83), following the procedure described in Figure 2. The parent mutants fold more slowly than the wild type (Jackson et al., 1993; N. el Masry, unpublished). The mutant fragment IV39CI-2(20–59) associates/folds with a second-order rate constant of (1.6 ± 0.1) × 10^3 s^{-1} M^{-1}, and SA31CI-2(20–59), with a second-order rate constant of (5.1 ± 0.7) × 10^2 s^{-1} M^{-1}, both considerably lower than wild type (3.7 × 10^3 s^{-1} M^{-1}). Nevertheless, if the slow first-order phase is an isomerization, this would not change on mutation. The rate constants obtained were 0.011 ± 0.001 s^{-1} for IV39CI-2(20–59) and 0.010 ± 0.001 s^{-1} for SA31CI-2(20–59), confirming the hypothesis.

DISCUSSION

The two fragments of CI-2, CI-2(20–59) and CI-2(60–83), associate to form a native-like structure (Prat Gay & Fersht, 1994). The magnitude of the change of fluorescence on association is similar to that of the refolding of intact CI-2. The refolding of intact CI-2 proceeds with three exponential phases: the major change in magnitude occurs at 53 s^{-1}, and the minor phases that result from *cis–trans* isomerization of peptidyl–prolyl bonds occur at 0.43 and 0.024 s^{-1} (Jackson & Fersht, 1991b).

The association/folding of the two fragments occurs via two phases. The minor phase at higher concentrations of

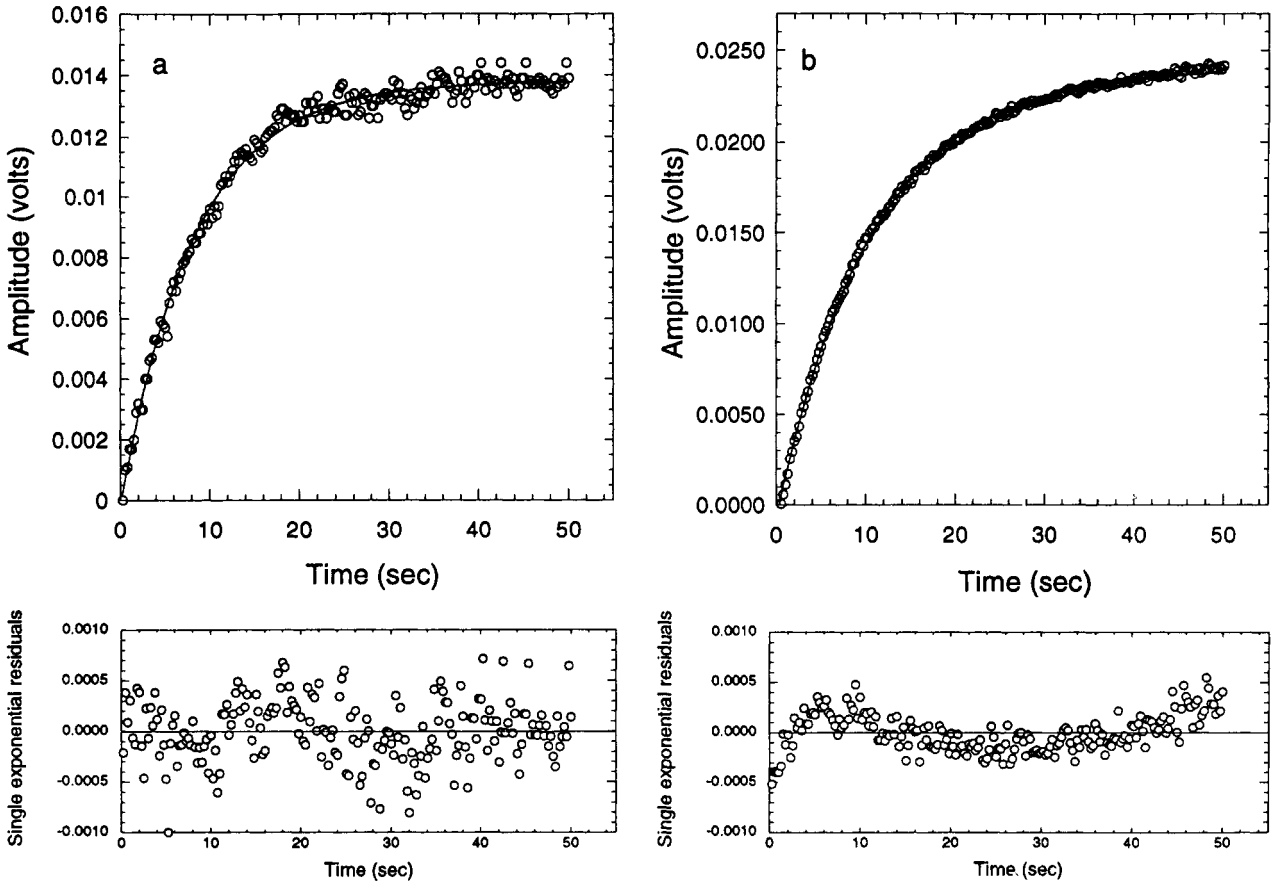

FIGURE 9: Pseudo-first-order association of fragments with CI-2(20–59) in excess of CI-2(60–83). The concentration ratios were (a) 25 μM:2.5 μM CI-2(20–59)/CI-2(60–83) and (b) 25 μM:2.5 μM CI-2(60–83)/CI-2(20–59). The increase in the signal in volts determined by the stopped-flow apparatus (see Experimental Procedures) corresponds to a decrease in fluorescence. Since CI-2(20–59) contains Trp-24, a high fluorescence background is present in panel a as well as photolysis; this was determined in a separate experiment and subtracted.

fragments proceeds at 0.01 s^{-1} and accounts for 20% of the amplitude. The faster phase, 80% of the amplitude at higher concentrations, follows second-order kinetics. The kinetic data are consistent with the mechanism

$$W_{major} + Y \underset{0.0004\ s^{-1}}{\overset{\sim 80\%\ 3700\ M^{-1}\ s^{-1}}{\rightleftarrows}} (W{\cdot}Y)_{folded}$$

$$\sim 20\% \downarrow\uparrow 0.011\ s^{-1}$$

$$W_{minor} + Y$$

where W is CI-2(20–59) containing Trp-24, major and minor refer to the phase which they produce, and Y is CI-2(60–83) containing Tyr-61.

Evidence from the double-jump experiment suggests the presence of a small (5%) population of fast-forming complex. This presumably corresponds to the amount of one or both fragments in a favorable conformation to yield a native-like complex.

The secondary and tertiary structures are formed cooperatively since the CD and fluorescence spectra are recovered concurrently. It thus appears that the second-order phase consists of an association step combined with a folding phase. Strong evidence to support this mechanism comes from examining the association of fragments derived from mutants of CI-2 that fold more slowly. The second-order rate constants for the association of the mutant fragments are correspondingly lower, whereas the slower first-order rate constant for the minor phase remains unaffected by mutation. The minor phase results from an isomerization in the CI-2(20–59) fragment since that step is seen only when an excess of CI-2(60–83) is mixed with CI-2(20–59) and not when a large excess of CI-2(20–59) is added to CI-2(60–83). This phase most probably results from an isomerization of one of the two proline residues (Pro-25 and Pro-44) in fragment CI-2(20–59). Pro-25 is in a turn next to Trp-24, and Pro-44 is located in a β-turn joining the α-helix with one of the β-strands.

The value of k_{off} could not be calculated accurately from pseudo-first-order rate constants, but can be calculated from the Gdm·Cl dissociation experiment (Figure 6). Using $K_D = k_{off}/k_{on}$, we obtain a value of 1×10^{-7} M for the K_D from kinetics, which is comparable to the value obtained at equilibrium, 0.4×10^{-7} M (Prat Gay & Fersht, 1994).

The association of the CI-2 fragments may be contrasted with the association of fragments of the ribonuclease barnase (Sancho & Fersht, 1992; Kippen *et al.*, 1994). Barnase is an α+β protein in which the elements of secondary structure are located on different halves of the polypeptide chain, so that the α-helices and the β-sheet may be separated in fragments. CI-2 is an α/β protein and, therefore, cleaved in two gives a fragment that contains the α-helix and strands of β-sheet. The helix-sequence-bearing fragment of barnase contains a few percent of α-helix, and the β-sequence-bearing fragments contain some preformed β-sheet (Kippen *et al.*, 1994). The rapid association of the barnase fragments with a second-order rate constant of $10^5\ s^{-1}\ M^{-1}$ most likely proceeds by the docking of preformed fragments; these could thus constitute initiation sites. The association of the two CI-2 fragments has a 25-fold lower second-order rate constant. The slower association presumably results from the β-structure not being

preformed since the β-strands are shared between the two fragments and the α-helix is not significantly formed in fragment CI-2(20–59) in solution (B. Davis, unpublished NMR data, and J. Ruiz-Sanz, unpublished CD data, this laboratory). There seem to be no well-defined initiation sites for the association/folding of CI-2 fragments compared to barnase; nevertheless, they associate tightly.

This reaction represents a folding process where the starting "unfolded" state is the fragments in water in the absence of denaturant. Further studies on the association of mutant fragments of CI-2 will allow the mechanism of folding complementation of the fragments to be established in a manner similar to that for intact barnase (Fersht, 1993).

REFERENCES

Brandts, J. F., Halvorson, H. R., & Brennan, M. (1975) *Biochemistry 14*, 4953–4963.

Dyson, H. J., Merutka, G., Waltho, J. P., Lerner, R. A., & Wright, P. E. (1992) *J. Mol. Biol. 226*, 795–817.

Fersht, A. R. (1985) *Enzyme Structure and Mechanism*, 2nd ed., W. H. Freeman, New York.

Fersht, A. R. (1993) *FEBS Lett. 325*, 5–16.

Gill, S. C., & von Hippel, P. H. (1989) *Anal. Biochem. 182*, 319–326.

Hartley, R. W. (1977) *J. Biol. Chem. 252*, 3252–3254.

Jackson, S. E., & Fersht, A. R. (1991a) *Biochemistry 30*, 10428–10435.

Jackson, S. E., & Fersht, A. R. (1991b) *Biochemistry 30*, 10436–10443.

Jackson, S. E., el Masry, N., & Fersht, A. R. (1993) *Biochemistry 32*, 11270–11278.

Karlplus, M., & Weaver, D. L. (1976) *Nature 260*, 404.

Kiefhaber, T., Grunert, U.-P., Hahn, U., & Schmid, F. X. (1990) *Biochemistry 29*, 6475–6479.

Kim, P. S., & Baldwin, R. L. (1990) *Annu. Rev. Biochem. 59*, 631–660.

Kippen, A. D., Sancho, J., & Fersht, A. R. (1994) *Biochemistry 33*, 3778–3786.

Laidler, K. J. (1950) *Chemical Kinetics*, Chapter 3, McGraw-Hill, New York.

Lang, K., Schmid, F. X., & Fischer, G. (1987) *Nature 329*, 268–270.

Levinthal, C. (1968) *J. Chem. Phys. 85*, 44–45.

Lin, L.-N., Hasumi, H., & Brandts, J. F. (1988) *Biochim. Biophys. Acta 956*, 256–266.

Prat Gay, G. de, & Fersht, A. R. (1994) *Biochemistry* (preceding article in this issue).

Ptitsyn, O. B. (1973) *Dokl. Akad. Nauk. 210*, 1213–1215.

Sancho, J., & Fersht, A. R. (1992) *J. Mol. Biol. 224*, 741–747.

Sancho, J., Neira, J. L., & Fersht, A. R. (1992) *J. Mol. Biol. 224*, 747–752.

Schmid, F. X. (1992) in *Protein Folding* (Creighton, T. E., Ed.) Chapter 5, W. H. Freeman, New York.

Shortle, D., & Meeke, A. K. (1989) *Biochemistry 28*, 936–944.

Taniuchi, H., & Anfinsen, C. B. (1971) *J. Biol Chem. 246*, 2291–2297.

Waltho, J. P., Feher, V. A., Merutka, G., Dyson, H. J., & Wright, P. E. (1993) *Biochemistry 32*, 6337–6347.

Wetlaufer, D. B. (1973) *Proc. Natl. Acad. Sci. U.S.A. 70*, 697–701.